Cytoplasmic short linear motifs in ACE2 and integrin β3 link SARS-CoV-2 host cell receptors to endocytosis and autophagy

Johanna Kliche, Muhammad Ali, Ylva Ivarsson *

Department of Chemistry, BMC, Uppsala University, Husargatan 3, 751 23 Uppsala, Sweden

Communicating author: ylva.ivarsson@kemi.uu.se

Muhammad Ali: 0000-0002-8858-6776
Johanna Kliche: 0000-0003-3179-4635
Ylva Ivarsson: 0000-0002-7081-3846

Key words

SARS-CoV-2 receptors, SLiMs, endocytosis, autophagy, ACE2, integrins, LIR, phospho-regulation, protein-protein interactions

One sentence summary

Affinity measurements confirmed binding of short linear motifs in the cytoplasmic tails of ACE2 and integrin β3, thereby linking the receptors to endocytosis and autophagy.

Abstract

The spike protein of the SARS-CoV-2 interacts with angiotensin converting enzyme 2 (ACE2) and enters the host cell by receptor-mediated endocytosis. Concomitantly, evidence is pointing to the involvement of additional host cell receptors, such as integrins. The cytoplasmic tails of ACE2 and integrin β3 contain a plethora of predicted binding motifs. Here, we confirm the functionality of some of these motifs through affinity measurements. The class I PDZ binding motif in the ACE2 cytoplasmic tail binds the first PDZ domain of the scaffold protein NHERF3. The clathrin-adaptor subunit AP2 µ2 interacts with an endocytic motif in the ACE2 with low affinity and the interaction is abolished by phosphorylation of Tyr781. Furthermore, the C-terminal region of integrin b3 contains a LC3-interacting region, and its interaction with ATG8 domains is enhanced by phosphorylation. Together, our data provides possible molecular links between host cell receptors and endocytosis and autophagy.

Introduction

A novel coronavirus, severe acute respiratory syndrome coronavirus 2 (SARS-CoV-2), was identified as the pathologic agent for an outbreak of pneumonia in Wuhan, China in December 2019 (1). The virus, which is causing the new lung disease termed coronavirus disease 19 (COVID-19), has infected 30.6 million people and claimed over 945,000 fatalities (09/2020). It is hence posing an immediate health and socioeconomic threat with worldwide impact (2). Understanding how the virus infects and replicates within the host cell is crucial for the development of novel targeted therapies.

SARS-CoV-2 employs the angiotensin converting enzyme 2 (ACE2) as a human host receptor for cell attachment and subsequent receptor-mediated endocytosis (3,4). Structural validation of the interaction has been provided by co-crystallisation of the receptor binding domain of the SARS-CoV-2 spike protein with the ACE2 ectodomain, as well as a cryo-EM structure with full-length ACE2 (5,6). However, analysis of *ACE2* expression across different human tissues revealed surprisingly poor expression in the lungs as compared to, for instance, high expression in the kidney and heart (7,8). The extreme damage that the virus can inflict on infected lungs indicates the requirement to use alternative receptors for host cell attachment and entry. In line, neuropilin-1, abundantly expressed in the olfactory epithelium, was shown to enhance SARS-CoV-2 infection and confirmed as receptor (9). The role of C-type lectins as potential interactors for the SARS-CoV-2 spike protein on innate immune cells has additionally been pointed out (10). Last, integrins have been proposed as candidate receptors due to the presence of a known integrin-binding RGD motif in the spike protein (11). In support, integrin mediated endocytosis is used by a variety of viruses for cell attachment as well as cell entry (12,13). While experimental validation is still awaiting, the structural feasibility of an ACE2-integrin interaction has been analysed (14). In addition, integrin tissue distribution matches SARS-CoV-2 tropism more closely, which includes functional importance of integrin β_1 expression on type 2 alveolar epithelial cells (15).

3

Furthermore, there are as of now two case reports of COVID-19 patients with concomitant multiple sclerosis background, who were treated with Natalizumab, an antibody effectively blocking integrin α_4 binding (16,17). Both reports support a positive correlation between Natalizumab treatment and mild COVID-19 progression.

Considerable research has been focused on the interaction between the SARS-CoV-2 spike protein and cell surface receptor proteins, particularly ACE2 (3,4,9–11). Further insight into the viral entry mechanism may be provided by investigating the downstream effects of the binding event. Taking a bioinformatical approach, Mészàros *et al.* (14) analysed the cytoplasmic tails of ACE2 and integrins and predicted them to contain a number of short linear motifs (SLiMs) that may link host receptor binding to endocytosis and autophagy. SLiMs are typically 3-10 amino acids long stretches found in the intrinsically disordered regions of the proteome. They may serve as binding sites and engage in dynamic protein-protein interactions (18). Well-known binding motifs include the class I PDZ (PSD-95/Dlg/ZO-1) binding motif (x[ST]xΦ-COO-, where x indicates any amino acid and Φ indicates a hydrophobic amino acid) that directs PDZ domain containing proteins to the C-terminal tails of targets (19), the AP2 μ2 binding endocytic motif (YxxΦ) (20), and the LC3-interacting region (LIR) motif, which mediates the interaction with the ATG8 domain containing proteins MAP1LC3s and GABARAPs in the phagophore membrane (21). Hence, SLiMs on the cytosolic side of the host receptor proteins may allow the recruitment of proteins that enable and mediate receptor and concomitant virus particle internalisation.

Mészàros *et al*. predicted ACE2 to contain binding motifs for AP2 μ2, NCK Src Homology 2 (SH2) domains as well as PDZ and phosphotyrosine binding (PTB) domains (Figure 1). These binding motifs, if functional, would act as molecular platforms linking the receptor to the various biological processes associated with the interacting protein domains. AP2 μ2, for example, is part of the clathrin-adaptor complex formed during clathrin-dependent endocytosis (22). Further, SH2 domains are known phospho-Tyr binders and NCK proteins are specifically involved in the organisation of the actin cytoskeleton (23).

PDZ and PTB domains, on the other hand, are well-established scaffolding domains implicated in the assembly of protein networks (24,25). In addition, Mészàros *et al*. proposed the presence of a phospho-modulated LIR autophagy motif in both ACE2 and the integrin β3 tail (14). If functional, such a motif would provide a link between the receptors, as well as the potential viral entry route to the endocytic-lysosomal pathway.

A ACE2 C-terminus

772- KARSGENP<mark>YASI</mark>DISKGEN<mark>NPGF</mark>QNTDDVQ<mark>TSF</mark>-COO-

B Integrin beta3 C-terminus

765- DTANNPLYKEATST<mark>FTNI</mark>TYRGT - COO-

Figure 1: Peptide sequences from the cytoplasmic tails from **A**: ACE2 and **B**: integrin β3. green: region containing predicted overlapping binding sites for NCK SH2 domain, the ATG8 domains of MAP1LC3As and GABARAPs and AP2 μ2; grey: predicted PTB binding site; orange: predicted class I PDZ binding site; blue: predicted ATG8 binding site in integrin β3.

Phosphorylation of Ser/Thr/Tyr residues may enable, disable or tune a given interaction (26,27). As elaborated by Mészàros *et al*., Tyr781 in the ACE2 tail has emerged as a reproducible phosphosite in high-throughput phosphoproteomics studies (14). In the case of the integrin β tails, it is well-established that phosphorylation regulates their interactions with adaptor and scaffold proteins, for instance allowing competitive binding of PTB domains (28). A bimolecular switch has been suggested in integrin β3, so that phosphorylation of Tyr773 enables binding of DOK1 PTB, whereas phosphorylation of Thr777 creates a 14-3-3 ζ binding site (29). Integrin β tails have moreover a Ser/Thr-rich sequence, that precedes the predicted LIR autophagy motif. The stretch has been proposed to be phosphorylated by Akt and PDK1 (28,30), which would likely modulate the proposed ATG8 domain binding. As rewiring of phospho-signalling has been found as one of the primary host responses to SARS-CoV-2 infection (31), it is important to explore the phospho-regulation of protein-protein interactions in relation to viral entry and hijacking of the cellular machinery.

In this study we set out to test predicted binding motifs in ACE2 and integrin β_3 (14) and the potential phospho-regulation of the interactions by affinity measurements.

5

To this end, we expressed and purified 18 protein domains, and determined affinities with synthetic peptides representing relevant cytoplasmic regions of the receptor tails. We find that the NHERF3 PDZ1 and SHANK1 PDZ domains bind to ACE2 C-terminus. We further confirm that AP2 μ2 binds the cytoplasmic region of ACE2 with low affinity and that the interaction is negatively affected by phosphorylation. Unfortunately, we could not evaluate the functionality of the proposed ACE2 LIR to its full extend due to technical issues. We confirm that the LIR in integrin β_3 binds the ATG8 domains of MAP1LC3s and GABARAPs and that the strength of the interaction is increased by ligand phosphorylation.

Taken together, we established the functionality of a subset of the bioinformatically predicted binding motifs, and shed light on the intracellular molecular recognition events that ACE2 and integrin β_3 engage in, which in a further perspective may contribute to the understanding of how SARS-CoV-2 enters the host cell. On a more general note, identification of a functional phospho-dependent LIR motif in the tail of integrin β_3 allows to critically link integrin signalling to autophagy.

Results

We aimed to test the predicted SLiMs in the cytoplasmic tails of ACE2 and integrin β3 for PDZ domains, PTB domains, the μ2 subunit from the clathrin-adaptor AP2 as well as ATG8 domains. We expressed and purified a representative collection of protein domains and used them to explore the affinities for synthetic peptides representing the proposed binding motifs (Figure 1). Affinities were determined by fluorescence polarisation (FP) using fluorescein (FITC)-labelled peptides as direct binders (saturation curves; K_D values) or reporters of binding (displacement curves; K_I values).

6

**NHERF3 PDZ1 and SHANK1 PDZ domains bind the ACE2 C-terminus**

The presence of a putative classical class I PDZ binding motif in the cytoplasmic tail of ACE2, prompted us to assess direct binding of the C-terminal region to a selection of seven PDZ domains (MAGI PDZ1, NHERF3 PDZ1 and PDZ2, SCRIB PDZ1, SHANK1 PDZ, SNTA1 PDZ and TAX1BP3 PDZ known to interact with class I PDZ binding motif (32), and found in proteins expressed in the lung based on Uniprot annotations.

The labelled C-terminal peptide of ACE2 (FITC-QNTDDVQTSF-COO-) was titrated with increasing concentrations of PDZ domains (Figure 2A). The change in FP signal upon ligand binding was measured and plotted against the protein concentration. Among the seven tested domains, five PDZ domains were classified as non-binders or low-affinity binders of ACE2 as there was no saturation within the tested concentration intervals (0-100 µM or 0-200 µM depending on protein domain). In contrast, the first PDZ domain of NHERF3 and SHANK1 PDZ domain were found to bind with relevant affinities (K_D values of 8 and 14 µM respectively; Figure 2A, Table 1).

The putative ACE2 PTB binding motif binds to the SNX17 FERM domain with low affinity

We next tested the interactions of the predicted PTB binding motif (NPxF) in the ACE2 C-terminal tail. We attempted to obtain saturation curves for the FITC-labelled ACE2 peptide containing the predicted motif (FITC-SKGENNPGFQNT-NH$_2$) and the PTB domains from three proteins (DOK1, IRS1 and FRS2), the PTB-like lobe of the FERM domains of TLN1 and TLN2, and the full FERM domain from SNX17 (Figure 2B). However, none of the tested domains were confirmed as high affinity binders of the ACE2 peptide (Figure 2B). The negative result with the DOK1 PTB domain is in agreement with the bioinformatic analysis, that suggested that the motif should be recognized by a different type of PTB domain (14). Given that there approximately 60 human proteins contain PTB domains (25), a systematic study of PTB domain specificities is needed for a comprehensive picture.

The most promising result was found for the interaction between the SNX17 FERM domain and the ACE2 peptide (Figure 2B), for which we estimate the K_D of to be in the range of 200-300 µM. The experiment was however hampered by the low solubility of the protein domain used. In line with this finding, we note that the SNX17 FERM domain bind to NPx(F/Y) containing peptides and has been crystallised in complex with the NPxF containing peptide of KRIT1 (33, 34). The ACE2 peptide thus matches its binding preference. An interaction between the SNX17 FERM domain appears reasonable given that the protein is involved in endosomal recycling of various proteins, including integrins (33,35).
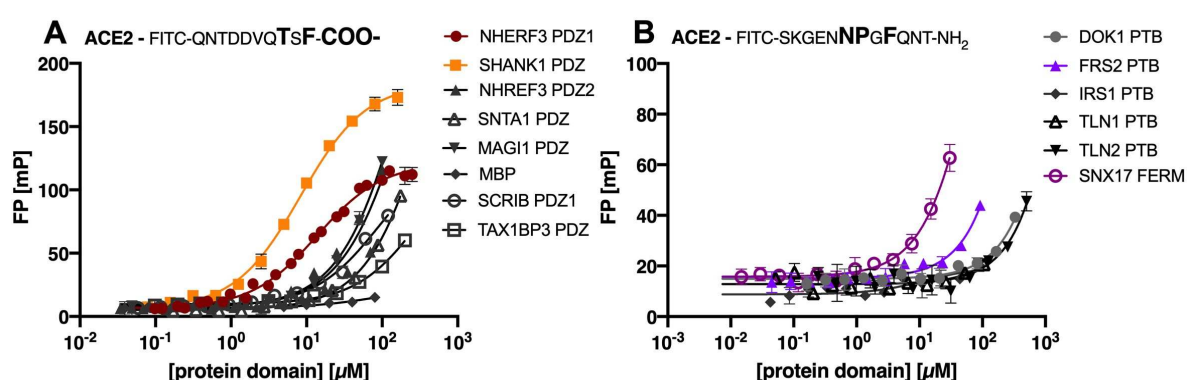
Figure 2: Saturation curves obtained by FP experiments for (**A**): selected class I PDZ domains and (**B**): a selection of PTB domains and SNX17 FERM. Curves were obtained by titrating the protein domains against the respective FITC-labelled ACE2 peptide, containing either a class I PDZ or a predicted PTB binding motif.

The ACE2 tail harbours a weak phospho-regulated AP2 µ2 binding motif

The ACE2 tail contains a nine amino acid stretch that is predicted to contain overlapping binding motifs for AP2 µ2, NCK SH2 and the ATG8 proteins (14). In addition, the region contains two phosphosites predicted to serve as bimolecular switches. We aimed at testing the interactions and the predicted phospho-switches in ACE2 binding by measuring the affinities of AP2 µ2, NCK1 SH2 and four ATG8 domains (MAP1LC3A, -B and -C, GABARAPL2) for unphosphorylated and phosphorylated (pTyr781 and pSer783) ACE2 peptides through peptide displacement experiments. Unfortunately, we were not able to determine the affinities for the pSer783 ACE2 peptide due to presence of contaminations that hindered accurate measurement despite ordering the peptide from two different companies.

8

First, saturation curves for the different protein domains with respective FITC-labelled probe peptides were obtained (Figure 3A, Table 2) to determine appropriate protein domain concentrations for displacement experiments. The labelled peptides for AP2 µ2 (ATG9A) and the ATG8 (SQSTM1) domains were chosen based on our unpublished proteomic peptide phage display data whereas the FITC-labelled peptide (Tir10) for NCK1 SH2 is a reported high-affinity binder (36). Subsequently, ACE2 peptides were titrated against the varying complexes of FITC-labelled peptide and protein domain (Figure 3B), from which IC50 values were derived and K_I values could be calculated. However, the ATG8 domains bound neither the unphosphorylated ACE2 nor pTyr781 peptide with relevant affinities (Figure 3B, estimated K_I values in mM range). In light of the fact, that the pSer783 peptide binding could not be assessed in the present study, we cannot rule out that the phosphosite interspersed in the predicted LIR motif may enhance affinity, which necessitates an alternative approach (e.g. direct binding with FITC-labelled ACE2 peptide).

The NCK1 SH2 did not bind to either of the tested peptides, which may reflect the difficulties in accurately predicting binding motifs of SH2 domains with relatively poorly defined consensus motifs. However, it should be noted that the predicted motif might serve as an interaction site for other SH2 domains. In contrast, we demonstrate a weak interaction between AP2 µ2 and ACE2 peptide with preferential binding to unphosphorylated ACE2 peptide (K_I value = 101 $\pm$ 5 µM). Phosphorylation at Tyr781 disabled the interaction with AP2 µ2, which is consistent with previous reports (37,38). We thus confirm the presence of a weak endocytic sorting signal in ACE2 C-terminal tail, that may be regulated by phosphorylation.
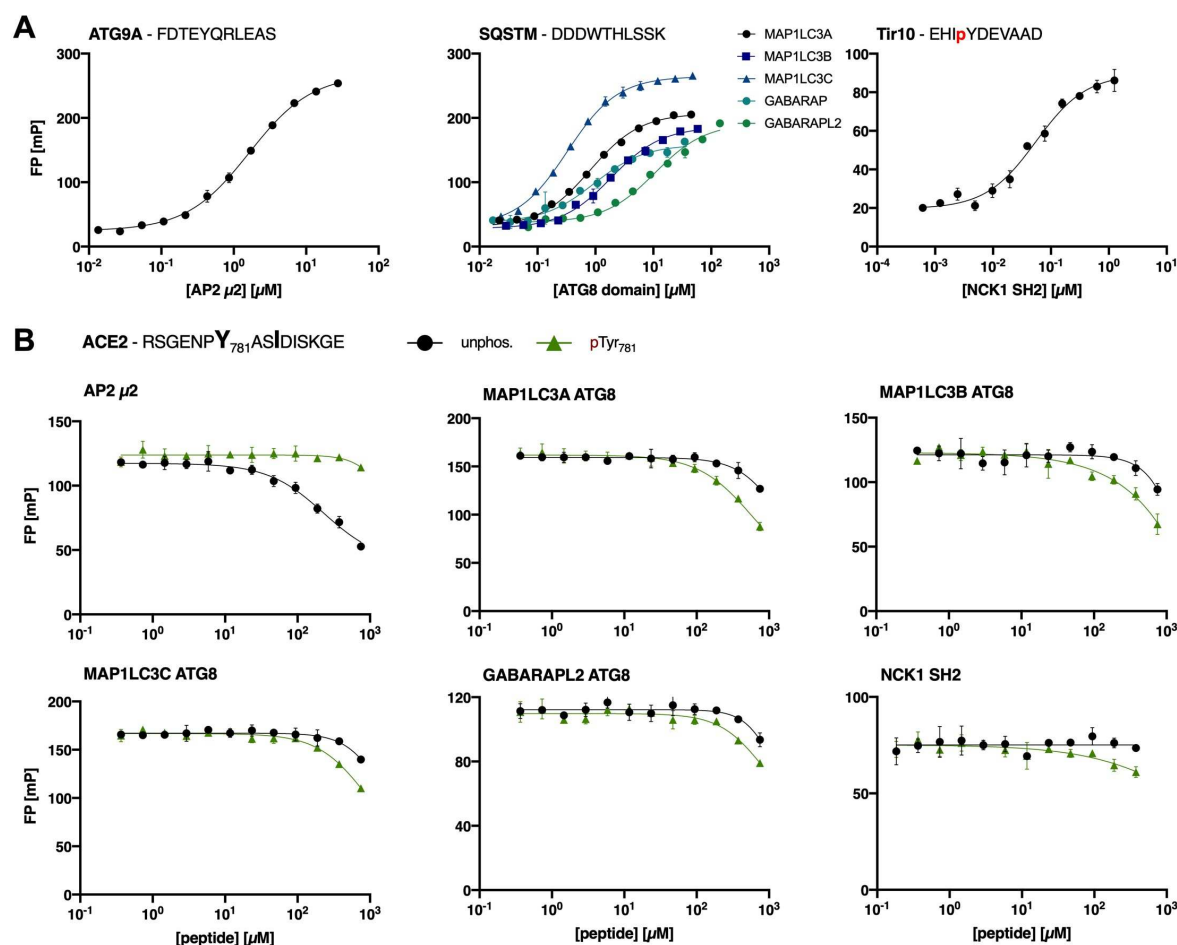
9

Figure 3: A: Saturation curves of AP2 μ2, the ATG8 domains and NCK1 SH2 for the respective FITC-labelled peptides (ATG9A, SQSTM1 and Tir10). **B**: Displacement curves of FP experiments using a peptide from the cytoplasmic ACE2 tail predicted to contain AP2 μ2, ATG8 and NCK SH2 domain binding motifs. Preferential binding of the different domains for unphosphorylated and pTyr781 ACE2 peptide was tested.

The integrin β₃ tail contains a phospho-regulated LIR motif

After the evaluation of the proposed SLiMs in the ACE2 tail we assessed the predicted LIR motifs in integrin tails, using the integrin β3 tail as a model system. We determined K_I values for unphosphorylated peptide as well as phospho-peptides spanning the region of the potential binding motif by displacement experiments. The hydrophobic motif is represented by Phe780 and Ile783 and interspaced by two variable amino acids (Figure 1). Preceding the motif, there is a Ser/Thr-rich sequence (residues 777-779), suggested to be subjected to phosphorylation. In context of the LIR motif, Tyr785 emerges equally as relevant potential phosphosite (14).

Displacement curves were obtained in the same fashion as described above and KI values concomitantly calculated (Figure 4, Table 3). We can in particular demonstrate that the interaction is tuned by phosphorylation of residues upstream and downstream of the core hydrophobic motif. We found that the unphosphorylated peptide is essentially not bound by the ATG8 domains tested. Phosphorylation of Ser778 located upstream of the hydrophobic motif strengthened ATG8 binding for all domains tested, while Thr779 phosphorylation enhanced the affinity for MAP1LC3C, but had no effect on the binding of the other ATG8 domains. Phosphorylation of the downstream residue Tyr785 conferred improved affinity in all tested cases. Concomitant phosphorylation of Thr779 and Tyr785 promoted ATG8 domain binding (double phosphorylated integrin β3 peptide) and increased the binding affinity of MAP1LC3C even further, indicating a synergistic effect of the two phosphosites (Figure 4). We thus clearly demonstrate a phospho-dependent interaction between the ATG8 proteins at the biophysical level.
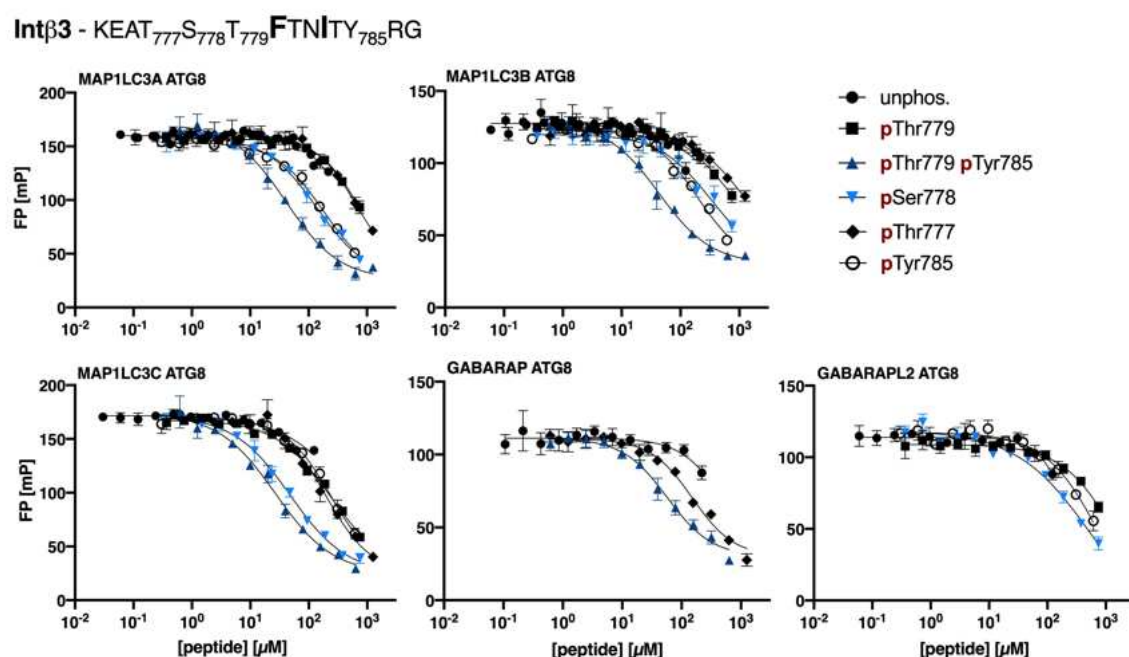
Figure 4: Fluorescence polarisation displacement curves obtained using unphosphorylated and phosphorylated peptides representing the cytoplasmic integrin β3 tail. Peptide sequence and sampled phosphosites are indicated in the figure.

Discussion

We provide biophysical evidence for the functionality of SLiMs harboured by the cytoplasmic tails of ACE2 and integrin β_3, providing possible links between the receptors and both endocytosis and autophagy.

Validation of trafficking motifs in the C-terminal tail of ACE2

Coronaviruses, including SARS-CoV-2, are proposed to utilise either the endocytic or non-endosomal pathway for cell entry (39). Our biophysical validation confirms the presence of an endocytic AP2 µ2 binding motif in the ACE2 C-terminus, which is negatively regulated by Tyr781 phosphorylation. This finding supports the possibility of clathrin-dependent endocytosis of SARS-CoV-2 upon receptor binding. However, it will of course be necessary to assess the biological relevance of the validated ACE2-AP2 µ2, particularly in light of its low affinity (100 µM). Concerning the latter, it can be noted that, while affinities of AP2 core complexes for endocytic sorting signals are reported in nanomolar range, measured K_D values of the AP2 µ2 subunit alone vary between 10 to 70 µM (40–42). Those reports contextualise the here reported affinity to a reasonable range.

Through our small-scale sampling, guided by tissue distribution and PDZ binding motif preferences, we demonstrate that SHANK1 PDZ and NHERF3 PDZ1 bind to the C-terminus of ACE2 with similar affinities. Between the two PDZ domains, the SHANK1 interaction appears less physiologically relevant because SHANK proteins have a known role in the structural organisation of the postsynaptic density (43). In contrast, NHERF3 serves as a scaffold protein that regulates the surface expression of plasma membrane proteins in the apical domain of epithelial cells (44,45), which agrees with the fact that ACE2 is found enriched on the apical surface of conducting airway epithelia (46). NHERF3 has moreover been reported to interact with the glutamate transporter excitatory amino acid carrier (47). This transporter harbours, apart from the PDZ binding motif and similar to ACE2, an endocytic sorting signal demonstrated to mediate AP2 µ2-dependent endocytosis.

Hence, it is possible that an equivalent mechanism orchestrates ACE2 surface stabilisation (PDZ-mediated) and internalisation (AP2-mediated). It appears feasible that the interaction between NHERF3 and ACE2 is functionally relevant due to their involvement in similar biological processes and suggested shared tissue distribution. Our analysis, even though limited by the set of PDZ domains tested, points towards a specificity of ACE2-PDZ interactions. However, we note that there are more than 260 human PDZ domains with partially overlapping specificities (32), and that other class I PDZ domains with similar binding preferences, such as the sorting nexin 27 (SNX27) PDZ domain, may also be physiological binders. SNX27, involved in retrograde transport from endosome to plasma membrane and hence in the recycling of internalised transmembrane proteins (48), was recently found as a host factor required for efficient entry of an engineered SARS-CoV-2 variant, the spike protein of which contains a deletion at the S1/S2 subunit cleavage site (49). Thus, it is plausible that SNX27 is involved in recycling ACE2 to the plasma membrane, which would in extension promote viral entry. Alternative methods, such as the hold-up assay against the full PDZ domain collection (50), may shed further light on the PDZ specificity profile of the ACE2 C-terminus in the future. Finally, in terms of the NPxF motif we find that the interaction with SNX17 FERM is the most promising lead, and note that SNX27 is involved in preventing lysosomal degradation of β integrins by binding to a NPxY motif in the cytoplasmic tails of β integrin (35).

Functional LIR motifs in integrin β3 as potential linkage of SARS-CoV-2 infection to autophagy

We confirm that the ATG8 domains (MAP1LC3A, -B, -C, GABARAP, -L2) bind the integrin β3 cytosolic tail in a phospho-dependent fashion. Phosphorylation upstream of the core LIR motif in the integrin β3 peptide enhanced ATG8 domain binding with a pronounced synergistic effect between the Thr779 and Tyr785 phosphosites. Notably, phospho-regulation of the LIR motif has already been suggested by various reports (51). Future systematic analysis of the effects of phosphosites relative to the core LIR motif will provide additional

13

details of the regulation. The functionality of the LIR binding motif in integrin β_3 provides a direct link between the receptor and the autophagic machinery, establishing a possible mechanism how SARS-CoV-2 could hijack this pathway for its propagation. This hypothesis appears particularly feasible in light of the fact that ATG8 domains act as adaptors recruiting LIR-containing proteins to phagosomal membranes (51).

How the autophagic machinery is deployed during coronavirus infection is still under debate with the majority of research conducted on viruses such as SARS-CoV and mouse hepatitis virus (39). Recent interest is driven by e.g. the finding that a number of inhibitors with impact on the autophagic flux reduce the cytopathic effect of SARS-CoV-2 infection in Vero-E6 cells (52). Further, a study repurposing approved compounds identified apilimod, a PIKfyve kinase inhibitor (53), as a potent inhibitor of viral replication in an ex vivo lung culture system (54). PIKfyve kinase activity has been linked to critical membrane trafficking events due to the generation of $PI(3,5)P_2$ (55) and its inhibition by apilimod to induce secretory autophagy (56). The data, which we provide here, may hence shed light on the interconnection between infection and the autophagic path. Redistribution of membranes important for viral replication, which might be suggested by apilimod treatment, may sensitively affect viral entry and replication. However, *in-cellulo* follow-up studies are required to test whether the virus deploys the potential protein-protein interactions of integrin β_3.

From a more general perspective, an inverse relationship between autophagy and integrin-dependent anchorage signalling has been proposed, implying that the autophagic machinery counteracts anoikis (detachment-induced apoptosis) (57). For instance, downregulation of integrin β_3 resulted in upregulation of autophagy markers (58). In line, it was observed that blockage of $\alpha_V\beta_3$ signalling results in inhibition of adhesion and concomitant activation of the autophagic machinery, manifested in increased MAP1LC3B expression (59). Conclusive evidence linking integrin signalling and autophagy has thus been gathered, whereas the molecular basis underlying vesicular rearrangements and the trafficking of integrins has not been established so far.

The phospho-dependence of the LIR motif, which we demonstrate here, might explain the conditional regulation of the interaction. Intriguingly, Shc has been identified as a key mediator of anoikis and deletion of its PTB domain to result in loss of anoikis activity (60). Further, binding of the PTB domain to the integrin β_3 tail is dependent on the phosphorylation of Tyr785 (61,62), whereas double phosphorylation of Thr779 and Tyr785 abolishes the interaction (30). As we could show that the double phosphorylation enables binding of MAP1LC3s and GABARAP synergistically, it can be hypothesised that the integrin β_3 tail serves as a molecular platform signalling for either the induction of anoikis or protective autophagy.

Conclusion

To conclude, we report on the functionality of some of the predicted binding motifs harboured by the cytoplasmic tail of ACE2 including a selective class I PDZ binding motif and a weak endocytic sorting signal. The presence of these motifs points to protein-protein interactions downstream of receptor binding, which may mediate internalisation. This might be relevant in context of both normal cellular physiology and SARS-CoV-2 infection. While we cannot confirm the presence of an autophagy LIR motif in the ACE2 tail, we clearly establish a phospho-dependent LIR motif in the integrin $\beta3$ tail. This provides the molecular link between integrin $\beta3$ and the autophagic pathway. The study opens the way to researching the mechanistic details of the interplay between autophagy and integrin-mediated signalling. It would be interesting to assess whether the remainder of the β-integrin tails contain phospho-modulated LIR motifs as well. At this point, the coupled involvement of both integrins and the autophagic process in SARS-CoV-2 biology still awaits experimental validation but one can hypothesise that our data contributes to the understanding how the virus might deploy autophagosomes for viral propagation. Contextualising the biological relevance of these confirmed SLiM-based interactions appears as the next logical step.

Material and Methods

Peptides

Peptides (Table 4) were obtained from GL Biochem (Shanghai, China) or Genecust (Boynes, France). FITC-labelled peptides were dissolved in DMSO, whereas unlabelled peptides were dissolved in 50 mM sodium phosphate buffer pH 7.4. Either 50 mM sodium phosphate buffer pH 7.4 or phosphate-buffered saline (PBS) pH 7.4 with 3 mM dithiothreitol (DTT) were used and supplemented with 0.05 % Tween for diluting labelled peptides during fluorescence polarisation experiments.

Protein expression and purification

Protein domains (Table 5) were expressed in E.coli BL21-Gold (DE3), grown in 2YT (10 g/L yeast extract, 16 g/L tryptone and 5 g/L NaCl) and induced at $OD_{600} = 0.7$ with 1 mM isopropyl β-D-1-thiogalatactopyranoside followed by 16 h incubation at 18 °C. All domains were glutathione-S-transferase (GST)-tagged, except for the PDZ domains, which were expressed with a maltose binding protein (MBP)-tag. The GST-tagged constructs were purified with glutathione beads (GE Healthcare), whereas ion metal affinity chromatography using Ni^{2+} beads (GE Healthcare) was used for PDZ domains. For affinity measurements, the GST tag was removed by thrombin or tobacco etch virus protease (SNX17 FERM) cleavage, whereas the fluorescence polarisation experiments of the PDZ domains were performed on the tagged protein domains. After purification, protein domains were dialysed in 50 mM sodium phosphate buffer pH 7.4 1 mM DTT or PBS pH 7.4 3 mM DTT (PDZ domains). For the complex in displacement experiments, proteins were supplemented with 0.05 % Tween.

Fluorescence polarisation experiments

FITC-labelled peptides were used as probes (excitation: 485 nm, emission: 535 nm) and the emitted light was measured in a SpectraMax iD5 Multi-Mode Microplate Reader (Molecular Devices) in order to calculate the mP signal. Experiments were performed at room temperature using non-binding black half area 96-well microplates (Corning®) (50 μL/well).

16

Saturation experiments were conducted using 5 nM FITC-labelled peptide and a dilution series of respective protein domain. Displacement curves were obtained by using a premixed complex of protein domain ([protein domain] = 1-2 fold K_D of FITC-labelled probe) and FITC-labelled peptide (10 nM) and a dilution series of displacing peptide. All measurements were in technical triplicates, except for MAP1LC3B and GABARAPL2 ATG8 domain binding to ACE2 pTyr785 peptide for which a duplicate of the displacement was recorded. Ki values were calculated as described elsewhere (63).

References

1. Zhu N, Zhang D, Wang W, Li X, Yang B, Song J, et al. A novel coronavirus from patients with pneumonia in China, 2019. N Engl J Med. 2020;

2. World Health Organization. Novel Coronavirus (COVID-19) Weekly Epidemiological Update. WHO (September 21). 2020.

3. Zhou P, Yang X Lou, Wang XG, Hu B, Zhang L, Zhang W, et al. A pneumonia outbreak associated with a new coronavirus of probable bat origin. Nature. 2020;

4. Hoffmann M, Kleine-Weber H, Schroeder S, Krüger N, Herrler T, Erichsen S, et al. SARS-CoV-2 Cell Entry Depends on ACE2 and TMPRSS2 and Is Blocked by a Clinically Proven Protease Inhibitor. Cell. 2020;

5. Shang J, Ye G, Shi K, Wan Y, Luo C, Aihara H, et al. Structural basis of receptor recognition by SARS-CoV-2. Nature. 2020;

6. Yan R, Zhang Y, Li Y, Xia L, Guo Y, Zhou Q. Structural basis for the recognition of SARS-CoV-2 by full-length human ACE2. Science (80-). 2020;

7. Li MY, Li L, Zhang Y, Wang XS. Expression of the SARS-CoV-2 cell receptor gene ACE2 in a wide variety of human tissues. Infect Dis Poverty. 2020;

8. Hikmet F, Mear L, Uhlen M, Lindskog C. The protein expression profile of ACE2 in human tissues. bioRxiv. 2020;

9. Cantuti-Castelvetri L, Ojha R, Pedro LD, Djannatian M, Franz J, Kuivanen S, et al. Neuropilin-1 facilitates SARS-CoV-2 cell entry and provides a possible pathway into

the central nervous system. bioRxiv. 2020;

10. Gao C, Zeng J, Jia N, Stavenhagen K, Matsumoto Y, Zhang H, et al. SARS-CoV-2 Spike Protein Interacts with Multiple Innate Immune Receptors. bioRxiv. 2020;

11. Sigrist CJ, Bridge A, Le Mercier P. A potential role for integrins in host cell entry by SARS-CoV-2. Antiviral Res. 2020;

12. Torres-Gomez A, Cabañas C, Lafuente EM. Phagocytic Integrins: Activation and Signaling. Frontiers in Immunology. 2020.

13. Hussein HAM, Walker LR, Abdel-Raouf UM, Desouky SA, Montasser AKM, Akula SM. Beyond RGD: virus interactions with integrins. Archives of Virology. 2015.

14. Mészáros B, Sámano-Sánchez H, Alvarado-Valverde J, Čalyševa J, Martínez-Pérez E, Alves R, et al. Short linear motif candidates in the cell entry system used by SARS-CoV-2 and their potential therapeutic implications. 2020 Apr 21 [cited 2020 Jul 6]; Available from: http://arxiv.org/abs/2004.10274

15. Plosa EJ, Benjamin JT, Sucre JM, Gulleman PM, Gleaves LA, Han W, et al. β1 Integrin regulates adult lung alveolar epithelial cell inflammation. JCI Insight. 2020;

16. Borriello G, Ianniello A. COVID-19 occurring during Natalizumab treatment: a case report in a patient with extended interval dosing approach. Mult Scler Relat Disord. 2020;

17. Aguirre C, Meca-Lallana V, Barrios-Blandino A, del Río B, Vivancos J. Covid-19 in a patient with multiple sclerosis treated with natalizumab: May the blockade of integrins have a protective role? Multiple Sclerosis and Related Disorders. 2020.

18. Davey NE, Van Roey K, Weatheritt RJ, Toedt G, Uyar B, Altenberg B, et al. Attributes of short linear motifs. Mol Biosyst. 2012;

19. Ivarsson Y. Plasticity of PDZ domains in ligand recognition and signaling. FEBS Letters. 2012.

20. Boll W, Ohno H, Songyang Z, Rapoport I, Cantley LC, Bonifacino JS, et al. Sequence requirements for the recognition of tyrosine-based endocytic signals by clathrin AP-2 complexes. EMBO J. 1996;

21. Sora V, Kumar M, Maiani E, Lambrughi M, Tiberti M, Papaleo E. Structure and Dynamics in the ATG8 Family From Experimental to Computational Techniques. Frontiers in Cell and Developmental Biology. 2020.

22. Kaksonen M, Roux A. Mechanisms of clathrin-mediated endocytosis. Nature Reviews Molecular Cell Biology. 2018.

23. Buday L, Wunderlich L, Tamás P. The Nck family of adapter proteins: Regulators of actin cytoskeleton. Cellular Signalling. 2002.

24. Lee HJ, Zheng JJ. PDZ domains and their binding partners: Structure, specificity, and modification. Cell Communication and Signaling. 2010.

25. Uhlik MT, Temple B, Bencharit S, Kimple AJ, Siderovski DP, Johnson GL. Structural and evolutionary division of phosphotyrosine binding (PTB) domains. Journal of Molecular Biology. 2005.

26. Tompa P, Davey NE, Gibson TJ, Babu MM. A Million peptide motifs for the molecular biologist. Molecular Cell. 2014.

27. Nishi H, Hashimoto K, Panchenko AR. Phosphorylation in protein-protein binding: Effect on stability and function. Structure. 2011;

28. Legate KR, Fässler R. Mechanisms that regulate adaptor binding to β-integrin cytoplasmic tails. Journal of Cell Science. 2009.

29. Chatterjee D, D'Souza A, Zhang Y, Bin W, Tan SM, Bhattacharjya S. Interaction Analyses of 14-3-3ζ Dok1, and Phosphorylated Integrin β Cytoplasmic Tails Reveal a Bi-molecular Switch in Integrin Regulation. J Mol Biol. 2018;

30. Kirk RI, Sanderson MR, Lerea KM. Threonine phosphorylation of the β3 integrin cytoplasmic tail, at a site recognized by PDK1 and Akt/PKB in vitro, regulates Shc binding. J Biol Chem. 2000;

31. Bouhaddou M, Memon D, Meyer B, White KM, Rezelj V V, Marrero MC, et al. The Global Phosphorylation Landscape of SARS-CoV-2 Infection. Cell [Internet]. 2020; Available from: http://www.sciencedirect.com/science/article/pii/S0092867420308114

32. Tonikian R, Zhang Y, Sazinsky SL, Currell B, Yeh JH, Reva B, et al. A specificity map

for the PDZ domain family. PLoS Biol. 2008;

33.   Ghai R, Bugarcic A, Liu H, Norwood SJ, Skeldal S, Coulson EJ, et al. Structural basis for endosomal trafficking of diverse transmembrane cargos by PX-FERM proteins. Proc Natl Acad Sci U S A. 2013;

34.   Stiegler AL, Zhang R, Liu W, Boggon TJ. Structural determinants for binding of sorting nexin 17 (SNX17) to the cytoplasmic adaptor protein Krev interaction trapped 1 (KRIT1). J Biol Chem. 2014;

35.   Steinberg F, Heesom KJ, Bass MD, Cullen PJ. SNX17 protects integrins from degradation by sorting between lysosomal and recycling pathways. J Cell Biol. 2012;

36.   Frese S, Schubert WD, Findeis AC, Marquardt T, Roske YS, Stradal TEB, et al. The phosphotyrosine peptide binding specificity of Nck1 and Nck2 Src homology 2 domains. J Biol Chem. 2006;

37.   Shiratori T, Miyatake S, Ohno H, Nakaseko C, Isono K, Bonifacino JS, et al. Tyrosine phosphorylation controls internalization of CTLA-4 by regulating its interaction with clathrin-associated adaptor complex AP-2. Immunity. 1997;

38.   Owen DJ, Evans PR. A structural explanation for the recognition of tyrosine-based endocytotic signals. Science (80-). 1998;

39.   Yang N, Shen HM. Targeting the endocytic pathway and autophagy process as a novel therapeutic strategy in COVID-19. International Journal of Biological Sciences. 2020.

40.   Grass I, Thiel S, Höning S, Haucke V. Recognition of a basic AP-2 binding motif within the C2B domain of synaptotagmin is dependent on multimerization. J Biol Chem. 2004;

41.   Höning S, Sosa M, Hille-Rehfeld A, Von Figura K. The 46-kDa mannose 6-phosphate receptor contains multiple binding sites for clathrin adaptors. J Biol Chem. 1997;

42.   Smith SM, Baker M, Halebian M, Smith CJ. Weak molecular interactions in clathrin-mediated endocytosis. Frontiers in Molecular Biosciences. 2017.

43.   Monteiro P, Feng G. SHANK proteins: Roles at the synapse and in autism spectrum

disorder. Nature Reviews Neuroscience. 2017.

44. Seidler U, Singh AK, Cinar A, Chen M, Hillesheim J, Hogema B, et al. The role of the NHERF family of PDZ scaffolding proteins in the regulation of salt and water transport: Lessons learned from knockout mice. Ann N Y Acad Sci. 2009;

45. Broadbent D, Ahmadzai MM, Kammala AK, Yang C, Occhiuto C, Das R, et al. Roles of NHERF Family of PDZ-Binding Proteins in Regulating GPCR Functions. In: Advances in Immunology. 2017.

46. Jia HP, Look DC, Shi L, Hickey M, Pewe L, Netland J, et al. ACE2 Receptor Expression and Severe Acute Respiratory Syndrome Coronavirus Infection Depend on Differentiation of Human Airway Epithelia. J Virol. 2005;

47. D'Amico A, Soragna A, di Cairano E, Panzeri N, Anzai N, Sacchi FV, et al. The surface density of the glutamate transporter EAAC1 is controlled by interactions with PDZK1 and AP2 adaptor complexes. Traffic. 2010;

48. Lauffer BEL, Melero C, Temkin P, Lei C, Hong W, Kortemme T, et al. SNX27 mediates PDZ-directed sorting from endosomes to the plasma membrane. J Cell Biol. 2010;

49. Zhu Y, Feng F, Hu G, Wang Y, Yu Y, Zhu Y, et al. The S1/S2 boundary of SARS-CoV-2 spike protein modulates cell entry pathways and transmission. bioRxiv. 2020;

50. Vincentelli R, Luck K, Poirson J, Polanowska J, Abdat J, Blémont M, et al. Quantifying domain-ligand affinities and specificities by high-throughput holdup assay. Nat Methods. 2015;

51. Johansen T, Lamark T. Selective Autophagy: ATG8 Family Proteins, LIR Motifs and Cargo Receptors. Journal of Molecular Biology. 2020.

52. Gorshkov K, Chen CZ, Bostwick R, Rasmussen L, Xu M, Pradhan M, et al. The SARS-CoV-2 cytopathic effect is blocked with autophagy modulators. bioRxiv : the preprint server for biology 2020.

53. Cai X, Xu Y, Cheung AK, Tomlinson RC, Alcázar-Román A, Murphy L, et al. PIKfyve, a class III PI Kinase, is the target of the small molecular IL-12/IL-23 inhibitor apilimod and a player in toll-like receptor signaling. Chem Biol. 2013;

54. Riva L, Yuan S, Yin X, Martin-Sancho L, Matsunaga N, Pache L, et al. Discovery of SARS-CoV-2 antiviral drugs through large-scale compound repurposing. Nature. 2020;

55. Hasegawa J, Strunk BS, Weisman LS. PI5P and PI(3,5)P2: Minor, but essential phosphoinositides. Cell Struct Funct. 2017;

56. Hessvik NP, Øverbye A, Brech A, Torgersen ML, Jakobsen IS, Sandvig K, et al. PIKfyve inhibition increases exosome release and induces secretory autophagy. Cell Mol Life Sci. 2016;

57. Vlahakis A, Debnath J. The Interconnections between Autophagy and Integrin-Mediated Cell Adhesion. Journal of Molecular Biology. 2017.

58. Zhu Y, Li L, Gong S, Yu Y, Dai H, Cai G, et al. β3-Integrin inhibits lipopolysaccharide-induced autophagy in cardiomyocytes via the akt signaling pathway. Cardiol. 2015;

59. Lino RLB, dos Santos PK, Pisani GFD, Altei WF, Cominetti MR, Selistre-de-Araújo HS. Alphavbeta3 integrin blocking inhibits apoptosis and induces autophagy in murine breast tumor cells. Biochim Biophys Acta - Mol Cell Res. 2019;

60. Ma Z, Myers DP, Ru FW, Nwariaku FE, Terada LS. p66Shc mediates anoikis through RhoA. J Cell Biol. 2007;

61. Deshmukh L, Gorbatyuk V, Vinogradova O. Integrin β3 phosphorylation dictates its complex with the Shc phosphotyrosine-binding (PTB) domain. J Biol Chem. 2010;

62. Cowan KJ, Law DA, Phillips DR. Identification of Shc as the primary protein binding to the tyrosine-phosphorylated β3 subunit of α(IIb)β3 during outside-in integrin platelet signaling. J Biol Chem. 2000;

63. Nikolovska-Coleska Z, Wang R, Fang X, Pan H, Tomita Y, Li P, et al. Development and optimization of a binding assay for the XIAP BIR3 domain using fluorescence polarization. Anal Biochem. 2004;

64. Stolz A, Putyrski M, Kutle I, Huber J, Wang C, Major V, et al. Fluorescence- based ATG 8 sensors monitor localization and function of LC 3/ GABARAP proteins . EMBO J. 2017;

65.   Duhoo Y, Girault V, Turchetto J, Ramond L, Durbesson F, Fourquet P, et al. High-throughput production of a new library of human single and tandem PDZ domains allows quantitative PDZ-peptide interaction screening through high-throughput holdup assay. In: Methods in Molecular Biology. 2019.

Acknowledgement

Funding

Author contributions

YI and JK conceived experiments. MA and JK performed experiments and analysed results. JK and YI wrote the manuscript. All authors approved the final version.

Author contributions

The authors declare no competing interests.

Tables

Table 1: Equilibrium dissociation constant (K_D) values of the tested PDZ domains for FITC-labelled ACE2 peptides. Indicated errors are the errors of the mean (SEM). N.B. indicates no or low affinity (K_D >100 µM).

Peptide sequence	Protein domains	
	Name	$K_D \pm$ SEM [µM]
ACE2_PDZ_FITC * FITC-QNTDDVQTSF-COO-	MAGI1 PDZ1	N.B.
	NHERF3 PDZ1	13.9 $\pm$ 0.3
	NHERF3 PDZ3	N.B.
	SCRIB PDZ1	N.B.
	SHANK1 PDZ	8.3 $\pm$ 0.2
	SNTA1 PDZ	N.B.
	TAX1BP3 PDZ	N.B.

* MBP was tested as control for binding (n.b.) due to the PDZ domains being MBP-tagged.

Table 2: Equilibrium dissociation constant (K_D) values of AP2 µ2, the ATG8 domains and NCK1 SH2 for the respective FITC-labelled peptides (ATG9A, SQSTM1 and Tir10). Indicated errors are the errors of the mean (SEM).

Peptide sequence	Protein domains	
	Protein domain	$K_D \pm$ SEM [µM]
ATG9A_FITC FITC-FDTEYQRLEAS-NH$_2$	AP2 µ2	1.6 $\pm$ 0.1
SQSTM1_FITC FITC-DDDWTHLSSK-NH2	GABARAP ATG8	0.9 $\pm$ 0.1
	GABARAPL2 ATG8	11 $\pm$ 1
	MAP1LC3A ATG8	1.9 $\pm$ 0.1
	MAP1LC3B ATG8	8.3 $\pm$ 0.2
	MAP1LC3C ATG8	0.33 $\pm$ 0.01
Tir10_FITC FITC-EHIpYDEVAAD-NH$_2$	NCK1 SH2	0.055 $\pm$ 0.006

Table 3: K_I values for ATG8 domains calculated from displacement experiments using unphosphorylated integrin β_3 peptide as well as phosphorylated peptides (pThr777, pSer778, pThr779, pTyr785 or pThr779 pTyr785). Indicated error is the error of the mean (SEM). N.B. indicates no or low affinity (Ki >100 μM). N.M. indicates not measured.

Peptide sequences	Ki values $\pm$ SEM [μM]				
	MAP1LC3A ATG8	MAP1LC3B ATG8	MAP1LC3C ATG8	GABARAPL2 ATG8	GABARAP ATG8
unphoshorylated H_3CO-KEATSTFTNITYRG- NH_2	N.B.	N.B.	N.B.	N.B.	N.B.
pThr777 H_3CO-KEApTSTFTNITYRG- NH_2	N.B.	N.B.	73 ± 4	N.M.	47 ± 3
pSer778 H_3CO-KEATpSTFTNITYRG- NH_2	29.4 ± 0.5	N.B.	16.1 ± 0.5	80 ± 5	N.M.
pThr779 H_3CO-KEATSpTFTNITYRG- NH_2	N.B.	N.B.	82 ± 3	N.B.	N.M.
pTyr785 H_3CO-KEATSTFTNITpYRG- NH_2	38 ± 2	81 ± 2	83 ± 4	89 ± 12	N.M.
pThr779 pTyr785 H_3CO-KEATSpTFTNITpYRG- NH_2	8.5 ± 0.5	15 ± 1	8 ± 2	N.M.	17.8 ± 0.8

Table 4: Sequences of peptides used in fluorescence polarisation experiment.

Name	Sequence
ACE2_PTB_FITC	FITC-SKGENNPGFQNT-NH_2
ACE2_PDZ_FITC	FITC-QNTDDVQTSF-COO-
ACE2 unphos.	H_3CO-RSGENPYASIDISKGE-NH_2
ACE2 pTyr781	H_3CO-RSGENPpYASIDISKGE-NH_2
ACE2 pSer783	H_3CO-RSGENPYApSIDISKGE-NH_2
ATG9A_FITC	FITC-FDTEYQRLEAS-NH_2
Intβ_3 unphos.	H_3CO-KEATSTFTNITYRG- NH_2
Intβ_3 pThr777	H_3CO-KEApTSTFTNITYRG-NH_2
Intβ_3 pSer778	H_3CO-KEATpSTFTNITYRG-NH_2
Intβ_3 pThr779	H_3CO-KEATSpTFTNITYRG-NH_2
Intβ_3 pThr779 pTyr785	H_3CO-KEATSpTFTNITpYRG-NH_2
Intβ_3 pTyr785	H_3CO-KEATSTFTNITpYRG-NH_2
SQSTM1_FITC	FITC-DDDWTHLSSK-NH_2
Tir10_FITC	FITC-EHIpYDEVAAD-NH_2

Table 5: Protein domains and the encoding plasmids Species is human unless otherwise stated.

Name	Plasmid
MAP1LC3A ATG8 (2-119)	pGEX-4T1
MAP1LC3B ATG8 (2-119)	pGEX-4T1
MAP1LC3C ATG8 (2-125)	pGEX-4T1
GABARAPL2 ATG8 (2-115)	pGEX-4T1
NCK1 SH2 (275-377)	pGEX-2T
MAGI1 PDZ1 (1-106)	pETM41
NHERF3 PDZ1 (2-107)	pETM41
NHERF3 PDZ2 (132-224)	pETM41
SCRIB PDZ1 (718-814)	pETM41
SHANK1 PDZ (655-761)	pETM41
SNTA1 PDZ (84-171)	pETM41
TAX1B3 PDZ (7-124)	pETM41
DOK1 PTB (151-256)	pH1003
FRS2 PTB (8-136)	pH1003
IRS1 PTB (157-267)	pH1003
TLN1 PTB (442-770)	pH1003
TLN2 PTB (309-401)	pH1003
mouse SNX17 FERM (109-388)	pMCSG10

Figure legends

Figure 1: Peptide sequences from the cytoplasmic tails from **A**: ACE2 and **B**: integrin β3. green: region containing predicted overlapping binding sites for NCK SH2 domain, the ATG8 domains of MAP1LC3As and GABARAPs and AP2 µ2; grey: predicted PTB binding site; orange: predicted class I PDZ binding site; blue: predicted ATG8 binding site in integrin β3.

Figure 2: Saturation curves obtained by FP experiments for (**A):** selected class I PDZ domains and (**B)**: a selection of PTB domains and SNX17 FERM. Curves were obtained by titrating the protein domains against the respective FITC-labelled ACE2 peptide, containing either a class I PDZ or a predicted PTB binding motif.

Figure 3: A: Saturation curves of AP2 µ2, the ATG8 domains and NCK1 SH2 for the respective FITC-labelled peptides (ATG9A, SQSTM1 and Tir10). **B**: Displacement curves of FP experiments using a peptide from the cytoplasmic ACE2 tail predicted to contain AP2 µ2, ATG8 and NCK SH2 domain binding motifs. Preferential binding of the different domains for unphosphorylated and pTyr781 ACE2 peptide was tested.

Figure 4: Fluorescence polarisation displacement curves obtained using unphosphorylated and phosphorylated peptides representing the cytoplasmic integrin β3 tail. Peptide sequence and sampled phosphosites are indicated in the figure.